Journal of Statistical Physics, Vol. 94, Nos. 1/2, 1999

Predicting Fiber Contact in a Three-Dimensional Model of Paper

D. J. Gates[1] and M. Westcott[1]

Received April 14, 1998; final September 9, 1998

We present a new methodology for the mathematical analysis of 3D paper structure and apply it to a model that can be simulated on a computer. We rigorously derive upper and lower bounds for fiber contact areas, and derive an approximation that is very close to values calculated from the simulations. The method involves the stochastic geometry and combinatorics of large numbers of randomly located sets, which quantify the interactions between fibers. The main calculation involves a sum resembling a partition function with many-body interactions of all orders.

KEY WORDS: Paper structure; fiber physics; relative bonded area; random sets; geometric probability.

1. INTRODUCTION

In common paper, about 1/4 to 1/2 of the total surface area of fibers is in mutual contact, i.e., closer than the wavelength of light. Inter-fiber contact area is important for several reasons. Contact areas do not scatter light and so influence the opacity of paper. Contact areas are potential sites for inter-fiber bonding, and degree of bonding influences the load distribution along fibers and hence paper stiffness.[(1)] Degree of bonding obviously influences paper strength. Indeed, bonded area appears explicitly in several formulae for paper stiffness and strength.[(1–3)] Fiber contact is also well correlated with paper density or porosity, and hence with permeability.

However there is currently no adequate theoretical predictor of fiber contact in terms of fiber properties and paper-making parameters, which very much limits the usefulness of formulae for paper stiffness and strength.

[1] CSIRO Mathematical and Information Sciences, Canberra ACT 2601, Australia; e-mail: David.Gates@cmis.csiro.au, Mark.Westcott@cmis.csiro.au.

0022-4715/99/0100-0031$16.00/0 © 1999 Plenum Publishing Corporation

The essential difficulty is the complexity of the 3D structure formed by the compacted random mat of deformed fibers.

Recently, fiber contact and other structural properties have been estimated via computer simulation of the 3D paper structure.[4–9] Fibers are laid down one by one on a flat base and flex so as to partially conform to previous fibers (Fig. 1). The base is a square with a large number of square cells, and the vertical coordinate is discrete, so there is a large 3D array of cells, or a 3D lattice.

We take fibers to be oriented only in the 2 orthogonal horizontal directions of the lattice. Niskanen *et al.*[6] deal mainly with this case, which they refer to as "orthotropic." Despite this simplification, the model shows most of the basic structural features, and gives results similar to more complex simulations.[5, 6] Our fibers are one cell wide and extend right across the square. In order to avoid edge effects, periodic boundary conditions are applied. Fibers have equal thickness of t vertical cells, where t can be any positive integer.

The flexing rule is that a fiber can make at most one vertical lattice step per horizontal lattice step. Otherwise each fiber is lowered as far as possible without penetrating other fibers. This leads to fibers forming ramp-like structures with segments of fixed slope. The flexing rule roughly imitates the response of fibers, having intrinsic stiffness, to cohesive forces and applied pressure. The resulting structure (Fig. 1) is vertically asymmetric, having a flat base, resembling a calendered surface, and a rough top.

Two orthogonal fibers cross in the manner of Fig. 2(a). Figures 2(b) and (c) are equivalent discrete representations. Real fibers are hollow tubes, which collapse to different degrees in different types of paper; this depends on how much the pulp has been processed and the fibers softened. Thus fiber width might be up to 5 times fiber height, so cell width might be up to $5t$ times cell height. However, it is evident that the most basic

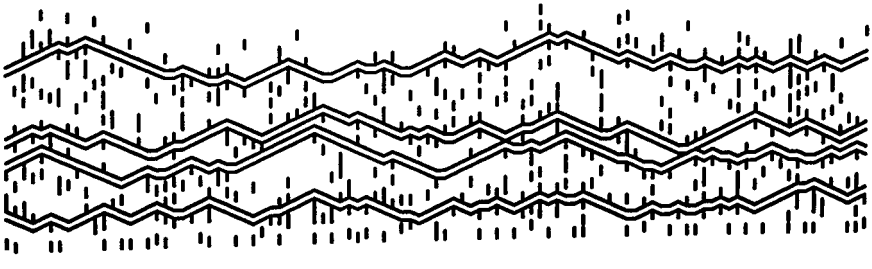

Fig. 1. Section view of a small "orthogonal fiber" simulation on a 100×100 base with 1000 fibers, each being a deformed rectangular rod 1 cell wide, 2 cells thick ($t = 2$) and extending right across the square. The 2 allowed fiber directions, parallel to the edges of the base, are equally probable.

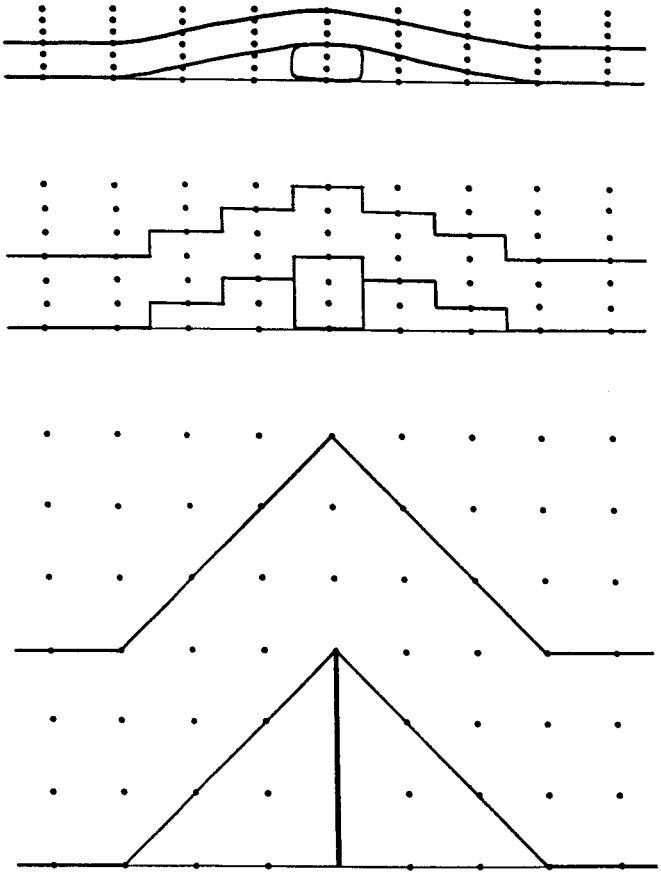

Fig. 2. (a) Sketch of a fiber bridging over another orthogonal to it on a flat base. (b) A discrete representation of (a) with fibers 1 cell wide and $t = 3$ cells high, as in Fig. 2 of ref. 6. (c) A convenient graphical representation equivalent to (b).

structural properties are independent of the vertical scale. All that matters is the value of t.

Although fibers are 1 cell wide, it is convenient to represent them graphically as single vertical planar strips centred on cells, as in Fig. 2(c). The upper fiber forms a ramp-like bridge over the lower one. The upper fiber fails to make contact with the base over an interval comprising $2t - 1$ cells. Evidently t is a natural indicator of fiber flexing. More generally, refs. 4–6 define a dimensionless fiber flexing number

$$F = \frac{\text{fiber width}}{t} \tag{1.1}$$

which is $1/t$ in our case. The structure formed by such fibers is determined entirely by F. Large F generates a dense structure while small F generates an open more porous structure. One could directly measure the F of real fibers via the Cyberflex apparatus[10] and use it to characterize the structure of real paper. Also, one can relate F to applied pressure and fiber stiffness using standard theory for the bending of beams.[10, 5]

Restricting fibers to width 1 implies a coarse discretization, and a limitation on possible fiber configurations. It also limits fiber flexibility, somewhat artificially, to values 1, 1/2, 1/3, etc.

Provided fiber length greatly exceeds t, length has negligible influence on paper structure. This would be true for real intact fibers; hence our fully spanning fibers. Real paper also contains small quantities of particles and fiber fragments, known as "fines." These are not included in the present model.

Fibers are deposited with angles randomly chosen from the 2 orthogonal directions with equal probability. The lateral coordinate of a fiber is uniformly random across the square. Figure 1 is a section view of a simulation with $t = 2$ and 1000 fibers on a 100×100 base There are 200 sections, so on average one would see only 5 fibers lying entirely in such a section. References 4 and 6 report extensive simulations and fitted curves for this model on a 1000×1000 base. Here we present some new simulations on a 5000×5000 base. Structural properties such as density and fiber contact are easily computed from the simulations.

The question we address here is: Can one predict mathematically the properties of such simulated paper, on average, without performing simulations? Even for our simple model, the 3D structure is immensely complex, and presents challenging mathematical problems. The methodology we present provides a means of tackling these problems, as well as more general paper structure. It involves the stochastic geometry and combinatorics of a large number of randomly located sets, which quantify the interactions between fibers.

Our mathematical predictions agree closely with our simulations. The main results are reported in Section 3, while Sections 4 to 8 contain the mathematics. Section 9 discusses some extensions of the present work.

2. INTER-FIBER CONTACT AND BASE-TO-FIBER CONTACT

Here we show how inter-fiber contact is related to contact area of fibers with the base, quantified by the *relative basal contact area*

$$\mathrm{RBCA} = |B|/|\Omega| \tag{2.1}$$

where Ω is the basal square (of cells), B the set of fiber surface (cells) in contact with Ω, and $|\ |$ indicates the area or number of cells in the set. RBCA is of structural interest in its own right since it measures the smoothness of the "calendered" surface, i.e., 1-RBCA is the proportion of imperfect or indented surface. The *relative contact area* (RCA) is the proportion of the total fiber surface area which is in mutual contact. It is related to RBCA as follows.

We notionally generate an independent but statistically identical simulation, invert it and place it in contact with the first on the common Ω. Then some of the contacts with Ω will become inter-fiber contacts. The combined structure has

$$\mathrm{RCA} = |C|/|A| \tag{2.2}$$

where A is the total fiber surface (we count the upper and lower surface of every fiber but not the vertical edges of the notionally rectangular fibers) and C is the subset of A where inter-fiber contacts occur (we count the contributions from both fibers in mutual contact). If D is any random surface with non-empty $A \cap D$, then

$$|C \cap D|/|A \cap D| \tag{2.3}$$

is an unbiased estimator of RCA. Hence

$$\widetilde{\mathrm{RCA}} = |C \cap \Omega|/|A \cap \Omega| \tag{2.4}$$

is an estimator of RCA, but may be biased because Ω is not randomly chosen and fibers cannot cross Ω. If the simulation below Ω makes fiber contact with Ω in a set B', then the total area of fiber in contact with Ω is $|A \cap \Omega| = |B| + |B'|$ and the total area of mutual fiber contact occurring on Ω is $|C \cap \Omega| = 2\,|B \cap B'|$. Thus

$$\widetilde{\mathrm{RCA}} = 2\,|B \cap B'|/(|B| + |B'|) \tag{2.5}$$

If the number of fibers in contact with Ω is large (as in our simulations) then these areas are close to their statistical means. The statistical independence of the upper and lower simulations implies that $|B \cap B'|$ has mean $b^2/|\Omega|$ where b is the mean of $|B|$ (or $|B'|$). Thus, as b, $|\Omega| \to \infty$ for fixed $b/|\Omega|$,

$$\widetilde{\mathrm{RCA}} \sim b/|\Omega| \sim \mathrm{RBCA} \tag{2.6}$$

because of (2.1).

Table I. Values of RCA and RBCA from Five Simulations with a Range of Values of t

t	1	2	3	5	10
RCA	0.607	0.417	0.273	0.177	0.096
RBCA	0.737	0.373	0.250	0.152	0.077

We performed some simulations to test this conclusion. The base was a 5000×5000 lattice. For each t we ran a long simulation with enough fibers to feel confident that the computed RCA had reached a stationary value. Basal contacts cease to be made much earlier in the simulations. Table I shows the results. These support (2.6), especially in the middle range 0.2 to 0.4 which is typical of real paper. We note that RCA > RBCA except in the case $t = 1$. This case is somewhat special; a fiber crossing another lying flat on the base can conform perfectly without leaving a gap. This plausibly has the effect of enhancing RBCA. These and other simulations are reported in more detail in Section 3. Our values of RCA are broadly consistent with the more complex simulations reported in ref. 6.

For thin paper, RCA is reduced because surface fibers have less contact area. In some applications, one is more interested in the RCA of fibers that are "internal" in some sense. Then D should be restricted to internal random surfaces, so RBCA has added plausibility as a measure of such an RCA.

3. THE MAIN RESULTS

As in ref. 6, one is interested in the dependence of paper structure on the *coverage* c, defined as the mean number of fibers vertically above a cell (in the Z direction). In our model $c = N/L$ for N fibers on a base of side L. In our simulations (and in real paper) N is large and the paper diameter L exceeds the fiber flexing distance t by many orders of magnitude. Consequently the mathematical regime of interest is $N, L \to \infty$ while $N/L \to c$ for fixed c and t. We write $\beta(c)$ for the RBCA in this regime. Here we quote our main results for $\beta(c)$ and compare them with simulations. Results for finite N and L and for Poisson N are given in later sections. We shall prove (Sections 4–7) that

$$\underline{\beta}(c) < \beta(c) < \bar{\beta}(c) \tag{3.1}$$

where

$$\bar{\beta}(c) = (1 - e^{-ct})/t \tag{3.2}$$

and

$$\underline{\beta}(c) = \begin{cases} c(1-ct) & \text{if} \quad c \leqslant 1/(2t) \\ 1/(4t) & \text{if} \quad c \geqslant 1/(2t) \end{cases} \tag{3.3}$$

In particular, for thick enough paper,

$$\frac{1}{4t} < \beta(\infty) < \frac{1}{t} \tag{3.4}$$

We also obtain the slightly better lower bound

$$\beta(c) > \beta_{-}(c) = \begin{cases} (2t - 2ct + 1)\, e^{c} - 2t - 1 & \text{if} \quad c \leqslant 1/(2t) \\ 2te^{1/2t} - 2t - 1 & \text{if} \quad c \geqslant 1/(2t) \end{cases} \tag{3.5}$$

For example, if $t = 1$ this gives $\beta(c) > 0.295$ for $c \geqslant 1/(2t)$, while (3.3) gives only $\beta(c) > 0.25$.

These results are obtained by a method involving the statistical geometry of regions of the base controlled by successive fibers. The regions

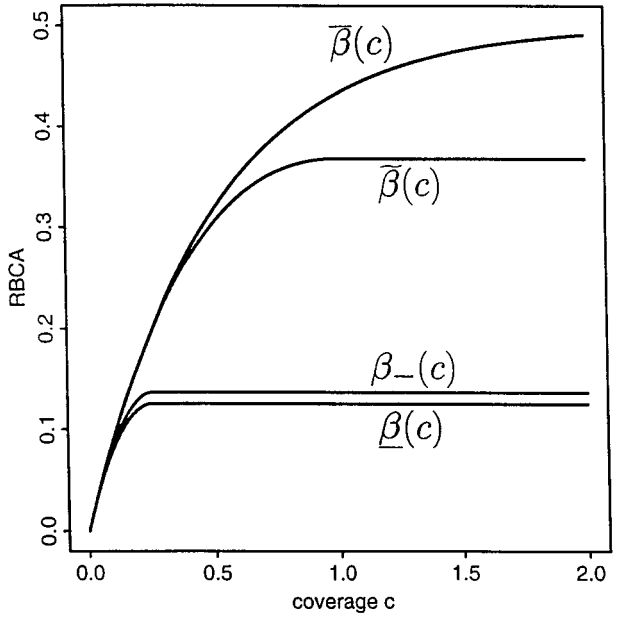

Fig. 3. The bounds $\bar{\beta}(c)$, $\underline{\beta}(c)$, $\beta_{-}(c)$ and the estimate $\tilde{\beta}(c)$ for the RBCA, given by Eqs. (3.1) to (3.6), plotted against the coverage c when $t = 2$.

Table II. Theoretical and Simulation Values of RBCA at Infinite Coverage for a Range of Values of *t*

t	1	2	3	5	10
$2/(et)$	0.7358	0.3679	0.2453	0.1472	0.0736
simulations 1	0.7366	0.3732	0.2502	0.1518	0.0768
simulations 2	0.7228	0.3663	0.2465	0.1498	0.0760
simulations 3	0.7278	0.3693	0.2465	0.1482	0.0747

are difficult to quantify exactly, but by using plausible estimates of their means we obtain (Section 8)

$$\beta(c) \simeq \tilde{\beta}(c) = \begin{cases} ce^{-ct/2} & \text{if} \quad c \leqslant 2/t \\ 2/(et) & \text{if} \quad c \geqslant 2/t \end{cases} \tag{3.6}$$

All these these results suggest that $\beta(\infty)$ is proportional to $1/t$, i.e., to the flexing number F. This may be compared with the simulations in ref. 6

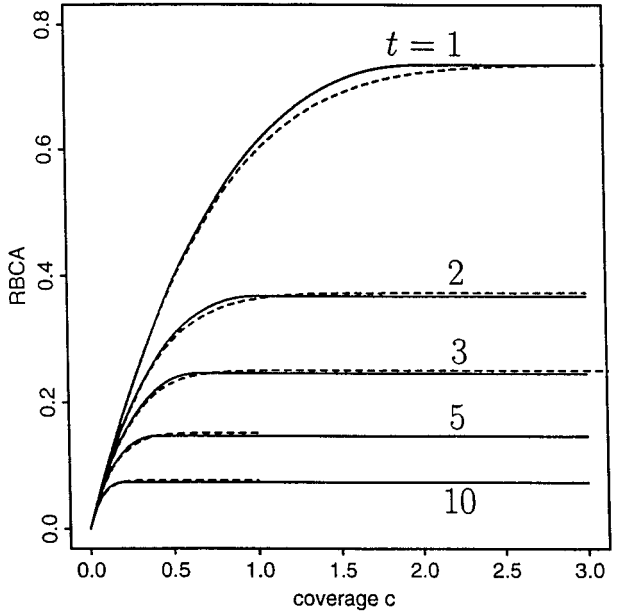

Fig. 4. Comparison of the predicted RBCA (solid lines) given by (3.6) with simulations (broken lines) of the orthogonal fiber model on a 5000×5000 base. Fibers have thicknesses of $t = 1$, 2, 3, 5, and 10, corresponding to flexing numbers 1, 1/2, 1/3, 1/5, and 1/10.

(their Fig. 3) though their fibers are not confined to width 1. Our Fig. 3 is a plot of these results against c for $t = 2$.

We compare $\tilde{\beta}(c)$ with simulations on a 5000×5000 grid (i.e., $L = 5000$). Each simulation was continued until one could be confident that no further basal contact would occur. Table II compares $2/(et)$ with computed $\beta(\infty)$ for 3 replicate simulations for a range of t values. Each of simulations i uses the same random number seed. Figure 4 shows plots of $\tilde{\beta}(c)$ against c, compared with the simulations 1, the others being very similar. Evidently $\tilde{\beta}(c)$ is an excellent approximation.

4. UPPER BOUND ON RBCA

When the first fiber is placed on the base it makes basal contact with a set $S(1)$ say of L cells. A second parallel fiber can make basal contact with L of the remaining $L(L-1)$ cells. But for a fiber orthogonal to the first, only $L(L-2t+1)$ sites are available; i.e., fiber 1 *obscures* a strip $2t-1$ cells wide from basal contact by any subsequent fibers orthogonal to it. We write $T(1, 2)$ for the set obscured from fiber 2 by fiber 1 in general. The basal contact of fiber number k is obscured in a complex way by fibers 1, 2,..., $k-1$, which will form a random stack in general. It is evident that the set obscured from k is at least as great as if fibers 1, 2,..., $k-1$ "ignored" each other and lay in perfect contact with the base. Thus the obscured set contains the set

$$T(1, k) \cup T(2, k) \cup \cdots \cup T(k-1, k) \tag{4.1}$$

where $T(j, k)$ is the set obscured from fiber k by fiber j alone, when j lies flat on the base. Thus, if fibers i and k are parallel, $T(i, k)$ is the set of basal cells in contact with fiber i; if they are perpendicular, $T(i, k)$ is a strip $2t-1$ wide around fiber i. If $S(k)$ is the set of L cells below fiber k, then the set $B(k)$ where fiber k makes basal contact satisfies

$$B(k) \subset S(k) \Big\backslash \bigcup_{i=1}^{k-1} T(i, k) \tag{4.2}$$

We define fiber i's position by an angle variable ϕ_i having two values (e.g., 0 for easterly and 1 for northerly) and the corresponding column or row number x_i with values 1, 2,..., L. We take the two angles to be equally probable and the x_i to be random and uniformly distributed on (1,..., L). We write $I(k) \equiv I(\phi_k, x_k, u, v)$ for the indicator function of $S(k)$, i.e., $I(k)$

takes value 1 if cell (u, v) lies in $S(k)$ but 0 otherwise. Also $J(i, k) \equiv J(\phi_i, x_i, \phi_k, x_k, u, v)$ denotes the indicator function of $T(i, k)$. Then we have

$$|B(k)| \leqslant \left| S(k) \Big\backslash \bigcup_{i=1}^{k-1} T(i, k) \right| = \sum_{u=1}^{L} \sum_{v=1}^{L} I(k) \prod_{i=1}^{k-1} [1 - J(i, k)]$$
$$= \bar{B}(k), \text{ say} \tag{4.3}$$

Denoting means over all the ϕ's and x's by $\langle\ \rangle$ and using the statistical independence of fibers, we have

$$\langle \bar{B}(k) \rangle = \sum_{u, v} \frac{1}{2} \sum_{\phi_k} \frac{1}{L} \sum_{x_k} I(k)[1 - \mathscr{T}(k)]^{k-1} \tag{4.4}$$

where

$$\mathscr{T}(k) \equiv \mathscr{T}(\phi_k, x_k, u, v) = \frac{1}{2} \sum_{\phi_i} \frac{1}{L} \sum_{x_i} J(i, k) \tag{4.5}$$

Now

$$J(i, k) = \begin{cases} 1 & \text{if} \quad \phi_i = \phi_k = 0 \text{ and } v = x_i \\ 1 & \text{if} \quad \phi_i = \phi_k = 1 \text{ and } u = x_i \\ 1 & \text{if} \quad \phi_i = 0,\ \phi_k = 1 \text{ and } x_i - t + 1 \leqslant v \leqslant x_i + t - 1 \\ 1 & \text{if } \phi_i = 1,\ \phi_k = 0 \text{ and } x_i - t + 1 \leqslant u \leqslant x_i + t - 1 \\ 0 & \text{otherwise} \end{cases}$$

Then for given ϕ_k, the sum contributes $2t - 1$ if fibers i and k are perpendicular and 1 if they are parallel; so, for all ϕ_k, x_k, u and v,

$$\mathscr{T}(k) = (2t - 1 + 1)/(2L) = t/L \tag{4.6}$$

Since

$$\sum_{u, v} I(k) = |S(k)| = L \tag{4.7}$$

we have

$$\langle \bar{B}(k) \rangle = L(1 - t/L)^{k-1} \tag{4.8}$$

and the upper bound on the mean RBCA for N fibers is

$$\frac{1}{L^2}\sum_{k=1}^{N}\langle \bar{B}(k)\rangle = [1-(1-t/L)^N]/t \tag{4.9}$$

For a Poisson number of fibers with mean cL this becomes $(1-e^{-ct})/t$, which is also the limit of (4.9) as $N, L \to \infty$ and $N/L \to c$. This proves (3.2).

5. COMBINED EFFECT OF OBSCURING SETS

To obtain our lower bounds and our approximation for RBCA we need to estimate the region or set on the base obscured from contact with fiber k due to the combined effect of fibers 1,..., $k-1$. Fibers 1,..., $k-1$ may form a complex stack, so their combined influence will be very complex. Finding a way of dealing adequately with this complexity is a basic problem in paper science. The following is a step in that direction. We formulate the method in terms of a lower bound on RBCA, but it also has application to the approximation (3.6) as described in Section 8.

From the previous section it is evident that

$$B(2) \supset S(2)\backslash T_1(1) \tag{5.1}$$

where $T_1(i) \equiv T_1(\phi_i, x_i)$ is a strip of width $2t-1$ around fiber i, *regardless* of the angle between fiber 1 and subsequent fibers. The region obscured from fiber 3 by fibers 1 and 2 is no greater than $T_1(1) \cup T_1(2)$ except in configurations where fiber 2 lies on top of and parallel to fiber 1, and fiber 3 bridges over the resulting barrier of height $2t$. Let $T_2(i) \equiv T_2(\phi_i, x_i)$ be a strip of width $4t-1$ around fiber i. In this particular configuration the obscured set is no larger than $T_2(1) = T_2(2) = T_2(1) \cap T_2(2)$. Thus in general

$$B(3) \supset S(3)\backslash W(1, 2) \tag{5.2}$$

where

$$W(i, j) = T_1(i) \cup T_1(j) \cup [T_2(i) \cap T_2(j)] \tag{5.3}$$

Now consider $B(4)$. Because fibers form linear "diagonal" bridges, one can see that if there is no square of side t that contains a segment of each of fibers 1, 2, and 3, then fibers 1, 2 and 3 obscure from 4 no more than every pair of fibers, i.e., no more than

$$W(1, 2) \cup W(1, 3) \cup W(2, 3) \tag{5.4}$$

If the fibers 1, 2 and 3 have a common point then they form simple structures that reach a height $3t$, and obscure no more than the further set

$$T_3(1) \cap T_3(2) \cap T_3(3) \tag{5.5}$$

where $T_3(i) \equiv T_3(\phi_i, x_i)$ is a strip of width $6t-1$ around fiber i. When fiber i is displaced from such a configuration the structure decreases in height, so fiber i's contribution to the obscured set is still less than $T_3(i)$. Thus the set obscured from fiber 4 never exceeds the union of (5.4) and (5.5), and so

$$B(4) \supset S(4) \backslash W(1, 2, 3) \tag{5.6}$$

where

$$\begin{aligned} W(i, j, k) = {} & T_1(i) \cup T_1(j) \cup T_1(k) \\ & \cup [T_2(i) \cap T_2(j)] \cup [T_2(i) \cap T_2(k)] \cup [T_2(j) \cap T_2(k)] \\ & \cup [T_3(i) \cap T_3(j) \cap T_3(k)] \end{aligned} \tag{5.7}$$

By similar reasoning one concludes that

$$B(k) \supset S(k) \backslash W(1,..., k-1) \tag{5.8}$$

where

$$W(1,..., j) = \bigcup_{E \subset (1,..., j)} \bigcap_{i \in E} T_{|E|}(i) \quad = \quad \bigcup_{r=1}^{j} \bigcup_{E \in \Lambda(r, j)} \bigcap_{i \in E} T_r(i) \tag{5.9}$$

where $T_r(i)$ is a strip of width $2rt-1$ around fiber i and $\Lambda(r, j)$ is the set whose elements are the r-member subsets of $(1, 2,..., j)$, e.g., $\Lambda(2, 3) = \{(1, 2), (1, 3), (2, 3)\}$. If $2(k-1)t-1 > L$ then T_{k-1} covers the base, so $W(1,..., k-1) = \Omega$ and the right side of (5.8) is empty. This reflects the fact that ultimately no more fibers can make contact with the base.

6. RECURRENCE RELATION FOR CONTACT AREAS

Having derived formulae for contact sets we now consider the areas of these sets. The developments in this section are essentially algebraic and combinatorial, and apply to more general models that lead to expressions of the form (5.8)–(5.9) with

$$T_r(i) \subset T_{r+1}(i) \qquad \text{for all } r, i \tag{6.1}$$

This could include fibers with real valued locations, arbitrary orientations and arbitrary lengths. Let $J_r(i) \equiv J_r(\phi_i, x_i, u, v)$ be the indicator function of $T_r(i)$. Then (5.8) gives

$$|B(k)| \geqslant \sum_{u,v} I(k)\, \Pi(k-1) = \underline{B}(k) \text{ say} \tag{6.2}$$

where

$$\Pi(j) = \prod_{r=1}^{j} \Phi_r(j) \tag{6.3}$$

is the indicator of $\Omega \backslash W(1,..., j)$,

$$\Phi_r(j) = \prod_{E \in \Lambda(r,j)} \Gamma_r(E) \tag{6.4}$$

and

$$\Gamma_r(E) = 1 - \prod_{i \in E} J_r(i) \tag{6.5}$$

There is a formal resemblance between $\Pi(j)$ and a Gibbs distribution for j particles. It involves r-body interactions $\Gamma_r(E)$ for all r, though the interactions operate only in the vicinity of point (u, v). Ultimately $\Pi(j)$ is summed over the fiber coordinates in the "partition function." (6.21). We now derive recurrence relations connecting the $\Pi(j)$. First

$$\Pi(k) = \Pi(k-1)\, F(k) \tag{6.6}$$

where

$$F(k) = \prod_{r=1}^{k} \prod_{E \in \Lambda(r-1, k-1)} \left[1 - J_r(k) \prod_{i \in E} J_r(i) \right] \tag{6.7}$$

To see this, consider just those factors in $\Phi_r(j)$ that involve $J_r(k)$. For any indicator functions G_α and H

$$\prod_{\alpha} (1 - HG_\alpha) = 1 - H + H \prod_{\alpha} (1 - G_\alpha) \tag{6.8}$$

Hence

$$F(k) = \prod_{r=1}^{k} [1 - J_r(k) + J_r(k)\, \Psi_r(k-1)] \tag{6.9}$$

where $\Psi_1 = 0$ and for $r > 1$

$$\Psi_r(j) = \prod_{E \in \Lambda(r-1,\, j)} \Gamma_r(E) \tag{6.10}$$

Now multiply out the product over r in $F(k)$. Since (6.1) implies $J_r(i)\, J_s(i) = J_r(i)$ for any $r < s$, we have

$$\prod_{r=1}^{s} [1 - J_r(k)] = 1 - J_s(k) \tag{6.11}$$

and therefore $F(k)$ reduces to

$$F(k) = \sum_{r=1}^{k-1} [J_{r+1}(k) - J_r(k)] \prod_{s=r+1}^{k} \Psi_s(k-1) + 1 - J_k(k) \tag{6.12}$$

Now multiply $\Pi(k-1)$ by $F(k)$ and note from (6.1) that

$$\Gamma_r(E)\, \Gamma_r(E') = \Gamma_r(E) \qquad \text{if} \quad E \subset E' \tag{6.13}$$

so that

$$\Phi_r(j)\, \Psi_r(j) = \Psi_r(j) \tag{6.14}$$

and that

$$\Gamma_{r-1}(E)\, \Gamma_r(E) = \Gamma_r(E) \tag{6.15}$$

so that

$$\Phi_{r-1}(j)\, \Psi_r(j) = \Psi_r(j) \tag{6.16}$$

Thus we find

$$\Pi(k) = \sum_{r=1}^{k-1} [J_{r+1}(k) - J_r(k)] \prod_{p=1}^{r-1} \Phi_p(k-1) \prod_{q=r+1}^{k} \Psi_q(k-1) + [1 - J_k(k)]\, \Pi(k-1) \tag{6.17}$$

One can regard $\Pi(j)$ as a function of the vector $\mathbf{T} = (T_1, ..., T_n)$ of all obscuring sets not larger than the base;

$$\Pi(j) \equiv \Pi_j(\mathbf{T}) \tag{6.18}$$

The suffix on Π_j indicates that it in fact depends only on $T_1,..., T_j$. Then $\Pi_j(T_{r_1},..., T_{r_n})$ means that $J_1,..., J_n$ are replaced by $J_{r_1},..., J_{r_n}$ in the definition of $\Pi(j)$. Thus we can write

$$\Pi_k(\mathbf{T}) = \sum_{r=1}^{k-1} [J_{r+1}(k) - J_r(k)]\, \Pi_{k-1}(\mathbf{T}\backslash T_r) + [1 - J_k(k)]\, \Pi_{k-1}(\mathbf{T}) \tag{6.19}$$

for $2kt - 1 < L$, while $\Pi_k = 0$ for larger k. We recall that Π_k is a function also of u, v and all of the ϕ_i and x_i for $i = 1,..., k$.

The lower bound $\underline{B}(k)$ has a statistical mean

$$\langle \underline{B}(k) \rangle = \sum_{u,\, v} \langle I(k)\, \Pi_{k-1}(\mathbf{T}) \rangle \tag{6.20}$$

It turns out that the mean

$$b_j = \langle \Pi_j(\mathbf{T}) \rangle = L^{-j} Q_j(\boldsymbol{\theta}) \tag{6.21}$$

depends only on $\boldsymbol{\theta} = (\theta_1,..., \theta_n)$, where $\theta_r = |T_r|/L$. In our specific model, $\theta_r = 2rt - 1$. Since Π_{k-1} involves only fibers $1,..., k-1$, and $I(k)$ involves only fiber k, the statistical independence implies

$$\langle \underline{B}(k) \rangle = \sum_{u,\, v} \langle I(k) \rangle\, b_{k-1} \tag{6.22}$$

Taking means of (6.19) and noting that $\langle J_r(i) \rangle = \theta_r/L$ we see that the "partition function" Q_j satisfies

$$Q_j(\boldsymbol{\theta}) = \sum_{r=1}^{j-1} (\theta_{r+1} - \theta_r)\, Q_{j-1}(\boldsymbol{\theta}\backslash\theta_r) + (L - \theta_j)_+\, Q_{j-1}(\boldsymbol{\theta}) \tag{6.23}$$

where $(x)_+ \equiv \max(x, 0)$. This equation implies that $Q_j = 0$ for $2jt - 1 > L$ without the need to specify any truncation. Since $Q_0 = 1$, the recurrence relation determines all the Q_j's. The relations imply that the Q_j are independent of u and v, so (6.22) reduces to

$$\langle \underline{B}(k) \rangle = L b_{k-1} \tag{6.24}$$

and so the mean RBCA has lower bound

$$\underline{\beta}_N = \frac{1}{L} \sum_{k=1}^{N} b_{k-1} \tag{6.25}$$

for N fibers. If N is a Poisson random variable with mean cL then the mean RBCA has lower bound

$$\underline{\beta}(c) = e^{-cL} \sum_{N=1}^{\infty} \frac{(cL)^N}{N!} \underline{\beta}_N = \int_0^c dc'\, e^{-c'L} \mathcal{Q}(c') \tag{6.26}$$

where

$$\mathcal{Q}(c) = \sum_{k=0}^{\infty} \frac{c^k}{k!} Q_k(\boldsymbol{\theta}) \tag{6.27}$$

is the "grand partition function."

The recurrence relation (6.23) implies that the Q_j have the form

$$Q_j(\boldsymbol{\theta}) = (L - \theta_j)_+ \, \hat{Q}_j(\boldsymbol{\theta}) \tag{6.28}$$

where the $\hat{Q}_j$ satisfy the similar recurrence relation

$$\hat{Q}_j(\boldsymbol{\theta}) = \sum_{r=1}^{j-1} (\theta_{r+1} - \theta_r)\, \hat{Q}_{j-1}(\boldsymbol{\theta} \backslash \theta_r) + (L - \theta_{j-1})\, \hat{Q}_{j-1}(\boldsymbol{\theta}) \tag{6.29}$$

with $\hat{Q}_1 = 1$. For example, $\hat{Q}_2(\boldsymbol{\theta}) = L + \theta_2 - 2\theta_1$ and

$$\begin{aligned} \hat{Q}_3(\boldsymbol{\theta}) = {} & (\theta_2 - \theta_1)(L + \theta_3 - 2\theta_2) + (\theta_3 - \theta_2)(L + \theta_3 - 2\theta_1) \\ & + (L - \theta_2)(L + \theta_2 - 2\theta_1) \end{aligned} \tag{6.30}$$

For general j there are 2^j linear equations for the same number of unknowns, corresponding to all the subsets of (1,..., j). Solving (6.29) for general θ_r's is a non-trivial task. We have written a computer program which computes the general solution up to $j = 21$ (using the FORTRAN limit of arrays with 20 indices). The program is useful for investigating contact areas of fibers that obey more realistic flexing rules, but the results are not presented in this paper.

Also, one can formally write down the general solution of (6.29). Let the j-vector $\mathbf{P}$ be a permutation of (1,..., j), and $\mathbf{P}_+$ the $(j+1)$-vector with first j elements given by $\mathbf{P}$ and last element L. Then

$$\hat{Q}_j(\boldsymbol{\theta}) = \sum_{\mathbf{P}} \prod_{r=1}^{j-1} (\theta_{m(r,\mathbf{P})} - \theta_r) \tag{6.31}$$

where the sum is over all permutations $\mathbf{P}$, and $m(r, \mathbf{P})$ is the smallest element in $\mathbf{P}_+$ that follows r and exceeds r. For example, if $j = 5$, $L > 5$ and

$\mathbf{P} = (3, 1, 5, 2, 4)$, then $m(1, \mathbf{P}) = 2$, $m(2, \mathbf{P}) = m(3, \mathbf{P}) = 4$ and $m(4, \mathbf{P}) = m(5, \mathbf{P}) = L$. For $Q_j(\boldsymbol{\theta})$ the product in (6.31) runs up to $r = j$ and $\theta_{m(j, \mathbf{P})} = L$.

7. THE LOWER BOUNDS

The simple lower bound (3.3) may be obtained by taking slightly larger sets T_r of width $2rt$ instead of $2rt - 1$. Then (6.29) reduces to

$$\hat{Q}_j(\boldsymbol{\theta}) = 2t \sum_{r=1}^{j-1} \hat{Q}_{j-1}(\boldsymbol{\theta} \backslash \theta_r) + [L - 2(j-1)\, t])\, \hat{Q}_{j-1}(\boldsymbol{\theta}) \tag{7.1}$$

with obvious solution $\hat{Q}_j(\boldsymbol{\theta}) = L^{j-1}$ for all j and $\boldsymbol{\theta}$. Thus

$$Q_j(\boldsymbol{\theta}) = L^{j-1}(L - 2jt)_+ \tag{7.2}$$

and so

$$\begin{aligned} \underline{\beta}_N &= \frac{1}{L} \sum_{j=0}^{N-1} (1 - 2jt/L)_+ \\ &= (N/L)[1 - t(N-1)/L] \qquad \text{if} \quad N \leqslant n(L) + 1 \end{aligned} \tag{7.3}$$

where $n(L)$ is the integer part of $L/(2t)$. If $N > n(L) + 1$, then

$$\underline{\beta}_N = [(n+1)/L][1 - nt/L] \geqslant 1/(4t) \tag{7.4}$$

In the limit $N, L \to \infty$, $N/L \to c$ this reduces to (3.3).

To derive the stronger lower bound (3.5) we use the values $\theta_r = 2rt - 1$. Then the recurrence relation (6.29) reduces to

$$\hat{Q}_j(\boldsymbol{\theta}) = \omega \sum_{r=1}^{j-1} \hat{Q}_{j-1}(\boldsymbol{\theta} \backslash \theta_r) + [L - \theta_1 - (j-2)\, \omega]\, \hat{Q}_{j-1}(\boldsymbol{\theta}) \tag{7.5}$$

where $\omega = 2t$. We have written the equation in this form in order to derive a more general solution, applicable in Section 8. The solution for each $\hat{Q}_j$ has the form

$$\sum_{i=0}^{j-1} c_{ij} (L - \theta_1)^i\, \omega^{j-i-1} \tag{7.6}$$

as one can verify by substitution. For $\theta_1 = \omega = 1$ (i.e., $t = 1/2$ in (7.1)) we know the solution

$$\hat{Q}_j(\boldsymbol{\theta}) = L^{j-1} = \sum_{i=0}^{j-1} c_{ij}(L-1)^i \tag{7.7}$$

for all L. This proves that the c_{ij} are the binomial coefficients $\binom{j-1}{i}$, and so the solution of (7.5) is

$$\hat{Q}_j(\boldsymbol{\theta}) = (L - \theta_1 + \omega)^{j-1} \tag{7.8}$$

Then substituting (6.28) for Q_j in (6.27) we have

$$\mathcal{Q} = \sum_{0 \leqslant k \leqslant v} \frac{[c(L-\eta)]^k}{k!} - c\omega \sum_{0 \leqslant k \leqslant v-1} \frac{[c(L-\eta)]^k}{k!} \tag{7.9}$$

where $\eta = \theta_1 - \omega$ and $v = (L-\eta)/\omega$. Thus

$$e^{-cL}\mathcal{Q} = e^{-c\eta}[P_v(v\zeta) - \zeta P_{v-1}(v\zeta)] \tag{7.10}$$

where $\zeta = c\omega$ and

$$P_v(z) = e^{-z} \sum_{0 \leqslant k \leqslant v} \frac{z^k}{k!} \tag{7.11}$$

is the Poisson cumulative distribution. If $L \to \infty$ then $v \to \infty$ and $P_v(v\zeta)$ concentrates on $\zeta = 1$, i.e.,

$$P_v(v\zeta) \to R(\zeta) = \begin{cases} 1 & \text{if} \quad \zeta < 1 \\ 1/2 & \text{if} \quad \zeta = 1 \\ 0 & \text{if} \quad \zeta > 1 \end{cases} \tag{7.12}$$

and likewise for $P_{v-1}(v\zeta)$. Thus

$$e^{-cL}\mathcal{Q} \to e^{-c\eta}(1-\zeta)\, R(\zeta) \tag{7.13}$$

and so (6.26) becomes

$$\beta_-(c) = \frac{1}{\omega} \int_0^m d\zeta (1-\zeta)\, e^{-q\zeta} \tag{7.14}$$

where $q = \eta/\omega$ and $m = \min(1, c\omega)$. Thus

$$\beta_-(c) = [1 - 1/q + (m + 1/q - 1)\, e^{-qm}]/\eta \tag{7.15}$$

For the case of current interest, $\eta = -1$ and $q = -1/(2t)$, which proves (3.5).

8. APPROXIMATION FOR THE CONTACT AREA

The lower bounds are based on sets T_r that significantly overestimate the obscuring effects. It seems clear that by correctly choosing the many-body interactions $\Gamma_r(E)$, one could write an exact formula for RBCA using our methodology. Then one could try to evaluate that formula. So far we have not succeeded with this difficult calculation. Instead we proceed by choosing T_r's that seem to be correct in an average sense.

First we note from Section 4 that a single fiber obscures on average an area $\mathscr{T}L^2 = tL$, so we choose a fixed T_1 of area tL, i.e. of width

$$\theta_1 = t \tag{8.1}$$

Figure 5 illustrates cases with larger r. Here we have r fibers crossing at the same point 0 and alternating in direction, with fiber r running up the page. They form a pyramid-like structure. The box represents the contribution $T_1 \cap \cdots \cap T_r$ (with our old T_i's) in our lower bound, added to the obscuring

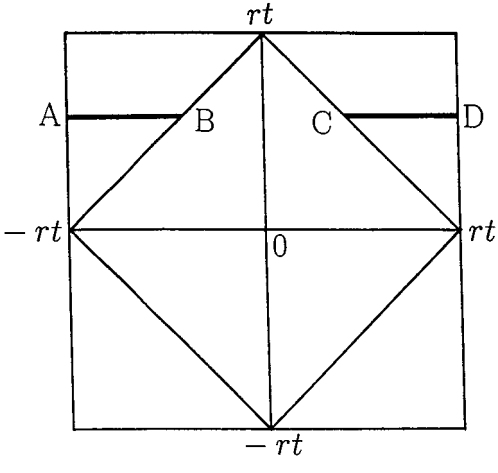

Fig. 5. The diagonally oriented square is a region of the base obscured by a stack of r fibers, crossing at the centre and alternating in direction, from an $(r+1)$th fiber, such as AD, orthogonal to fiber r.

set when fiber r is added to fibers 1,..., $r-1$. In reality, a new fiber AD, running across the page, is obscured only over the interval BC. Since AB crosses at a random uniform Y coordinate, the mean obscured distance is rt. A fiber crossing in the other direction is obscured by fiber r only if it lies on top thereof, so the obscured distance is $2rt$ with probability $1/(2rt)$, which contributes only 1 on average. Thus the obscuring effect of fiber r, on average, is approximated by a strip T_r of width $\frac{1}{2}rt$ for large r. With (8.1) this suggests we take

$$\theta_r = \tfrac{1}{2}(r+1)\, t \tag{8.2}$$

Now we have the recurrence relation (7.5) with $\omega = \frac{1}{2}t$. The solution (7.15) with $\eta = \frac{1}{2}t$, $q = 1$ and $m = \min(1, \frac{1}{2}ct)$ reduces to

$$\tilde{\beta}(c) = (2/t)\, me^{-m} \tag{8.3}$$

which establishes (3.6). For fixed N, summing (6.25) directly gives the rather simple result

$$\tilde{\beta}_N = (N/L)(1 - \tfrac{1}{2}t/L)^{N-1} \tag{8.4}$$

for $N \leqslant 2L/t$.

9. EXTENSIONS OF THE PRESENT WORK

Our results for RBCA, summarized in Section 3, show that our new methodology can make significant predictions about 3D simulated paper. We shall present predictions for paper volume, hence density or porosity, in a future paper. It would be valuable to apply the methodology to more realistic simulation models, leading one to make more confident predictions about real paper. Desirable extensions include:

(a) Orthogonal fibers with one direction preferred, imitating the influence of machine direction.

(b) Fibre width greater than one cell, i.e. a finer discretisation.

(c) Fibres with all possible orientations.

(d) Fibres of finite length and mixed lengths.

(e) Fibres with more realistic flexing behaviour.

Regarding (e), one would want to improve on the ramp-like bridges and structures evident in Fig. 1. A natural improvement is to constrain

fiber curvature rather than fiber slope. Or one might use a flexing rule that is consistent with the bending of beams.[10, 5] This would involve significant modifications of the simulation programs.

The mathematical methodology, however, lends itself readily to different flexing behaviour. One needs only to specify appropriate sets T_r in (5.8). For example, the deflection of a beam under uniformly distributed pressure is proportional to the 4th power of its length, so one could take θ_r increasing like $r^{1/4}$ (rather than r). In this case we have no simple solution of the recurrence relations (6.23). Fortunately the sums (6.25) and (6.27) for RBCA converge very fast for such θ_r, so the Q_j are needed only for small j, say $j \leqslant 10$. These can be computed in a few seconds.

The flexing behaviour of fibers in real paper might be more complex. Fibres might be constrained lengthwise in the forming paper, and so resist flexing. The beam bending mechanism is an assumption rather than an established fact. The true flexing principle is clearly of central interest, and needs to be clarified by observation.

ACKNOWLEDGMENT

We thank R. E. Johnston for bringing ref. 6 to our attention and for helpful conversations, and E. K. O. Hellén for bringing refs. 7 and 8 to our attention. This work began when DJG was a member of the CRC for Hardwood Fibre and Paper Science, which is funded by the Australian Federal Government.

REFERENCES

1. D. H. Page and R. S. Seth, The elastic modulus of paper. II. The importance of fiber modulus, bonding and fiber length, *Tappi Journal* **63**:113 (1980).
2. D. H. Page, A theory for the tensile strength of paper, *Tappi Journal* **52**(4):674 (1969).
3. P. P. Kärenlampi, The effect of pulp fiber properties on the tearing work of paper, *Tappi Journal* **79**(4):211 (1966).
4. K. J. Niskanen and M. J. Alava, Planar random fiber networks with flexible fibers, *Phys. Rev. Lett.* **73**(25):3475 (1994).
5. D. J. Gates, Simulating the three dimensional structure of paper. I. Influence of fibre length and fibre flexibility, *The CRC for Hardwood Fiber and Paper Science* (APPI, Monash University, Australia, 1996).
6. K. A. Niskanen, N. Nilsen, E. Hellén, and M. J. Alava, KCL–PAKKA: Simulation of the 3D structure of paper, p. 1273. In *Fundamentals of Paper Making Materials; Transactions of the 11th Fundamental Research Symposium, Cambridge*, C. F. Baker, ed. (PIRA International, 1997).
7. E. K. O. Hellén, M. J. Alava, and K. J. Niskanen, Porous structure of thick fiber webs, *J. Appl. Phys.* **81**(9):6425 (1997).

8. A. Koponen, D. Kanahai, E. Hellén, M. Alava, A. Hoekstra, M. Kataja, K. Niskanen, P. Sloot, and J. Timonen, Permeability of three-dimensional random fiber webs, *Phys. Rev. Lett.* **80**(4):716 (1990).
9. N. Nilsen, M. Zabihian, and K. Niskanen, KCL–PAKKA: A tool for simulating paper properties, *Tappi Journal* **81**(5):163 (1998).
10. R. Steadman and P. Luner, The effect of wet fiber flexibility on sheet apparent density, *Proc. 1985 Papermaking Raw Materials (Trans. 8th Fundamental Research Symposium) England*, Vol. 1, pp. 311–337 (1985).